

Supplementary Information

Highly efficient rGO-MoS₂ nanohybrid based laccase biosensor for hydroquinone detection in waste water

Sakshi Verma, Chandra Mouli Pandey, D Kumar

Figure S1. UV visible spectra of (i) GO and (ii) rGO-MoS₂

Figure S2. (A) Adsorption studies of 10 ppm MB under 2.5mg of rGO-MoS₂ nanocomposite using UV-Visible spectroscopy (B) Pseudo first order kinetics plot (C) Temkin adsorption isotherm plot (D) Freundlich adsorption isotherm plot

Figure S3. Zeta potential distribution of rGO-MoS₂ nanocomposite in DI

Figure S4. Comparison between CV (i) rGO-MoS₂/ITO (ii) GO/ITO (iii) Lac/rGO-MoS₂/ITO electrode and (iv) Hq/Lac/rGO-MoS₂/ITO electrode measured at 50 mV/s in PBS consisting of 5mM [Fe(CN)₆]³⁻ and [Fe(CN)₆]⁴⁻

Figure S5. Variation of concentration of Lac enzyme immobilized onto rGO-MoS₂/ITO for 100 μM Hq using Chronoamperometry

Figure S6. Variation of pH for PBS buffer for biosensing of 100 μM Hq using Chronoamperometry

Figure S7. Reproducibility of the fabricated biosensor at 100 μM Hq

Table 1. Comparison of adsorption capacity of different materials towards MB dye

Table 2. Feasibility of adsorption equations and isotherms towards adsorption of MB dye using rGO-MoS₂ with other parameters

Fig.S1

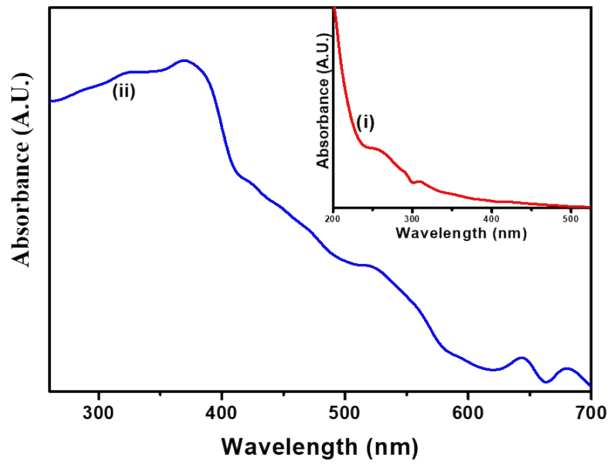


Fig.S2

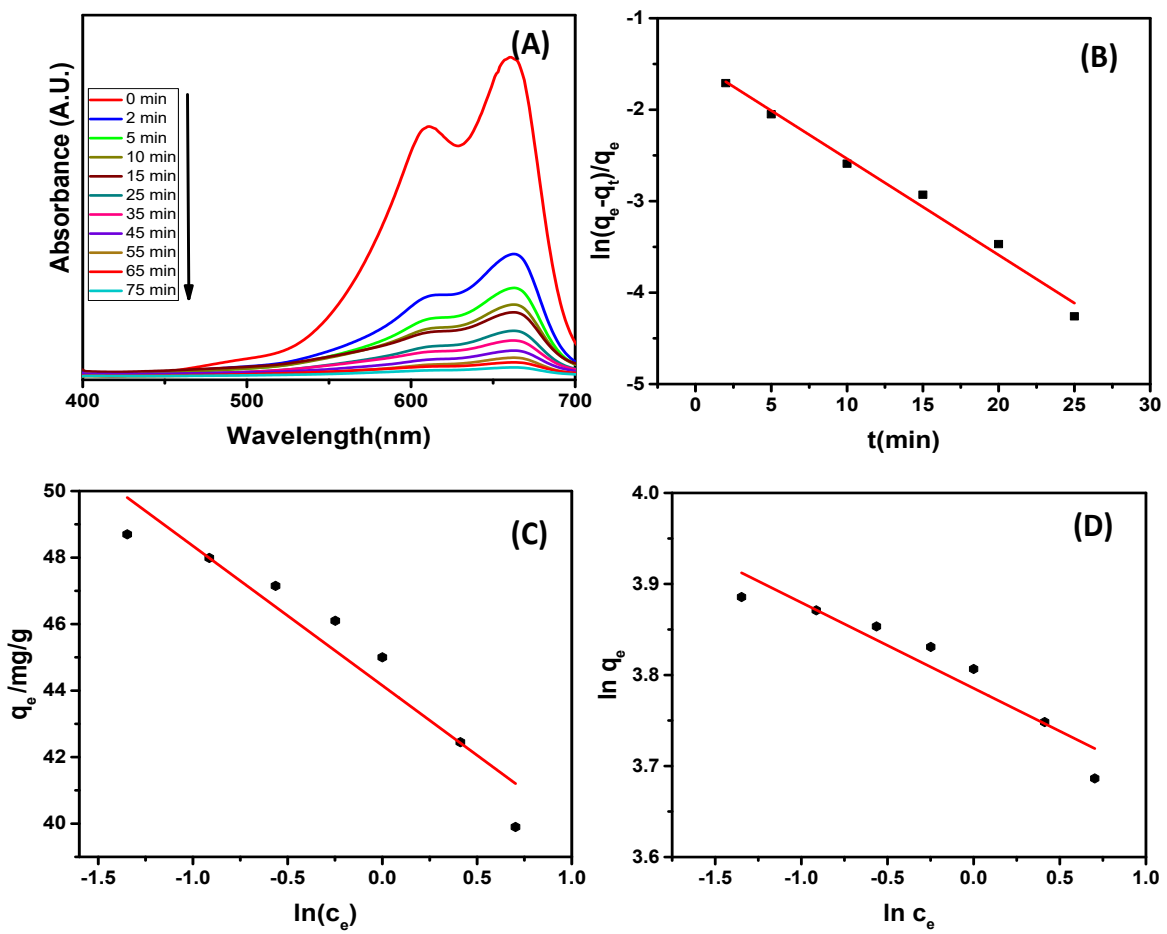


Fig.S3

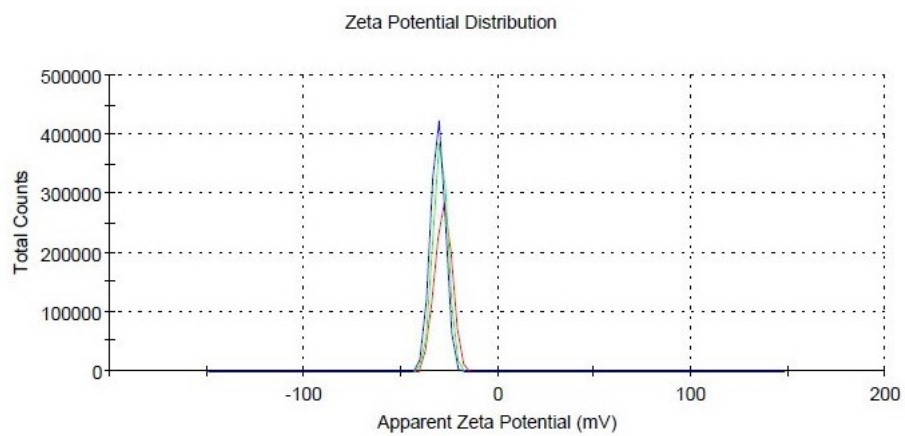


Fig.S4

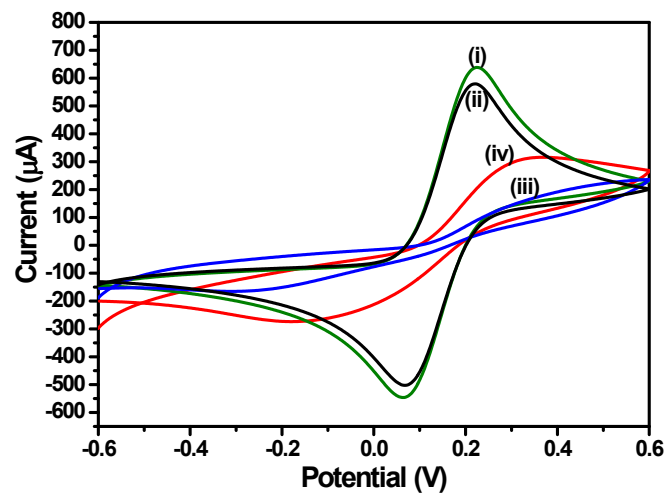


Fig.S5

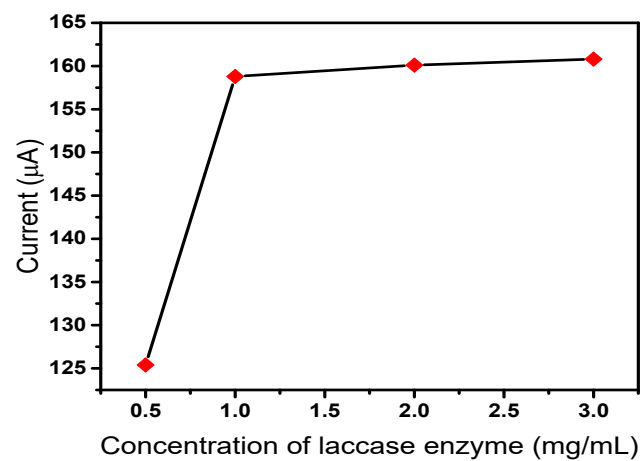


Fig.S6

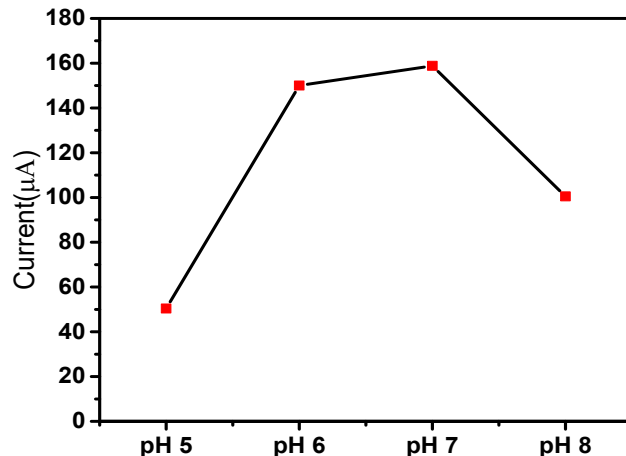


Fig.S7

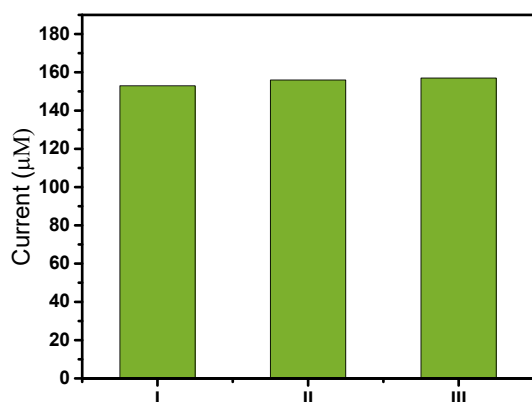


Table S1.

Adsorbent	Adsorption capacity	Concentration of MB	Reference
CNT	35.4 mg/g	20 ppm	[1]
Graphene	39.92 mg/g	20 ppm	[2]
Equations KMg ₂ Fe(PO ₄) ₂ Pseudo first order	R ² value 22.83 mg/g 0.986	Other Parameter 10 ppm	Value [3]
Electrolytic Pseudo second manganese anode order slime	70.74 mg/g 0.999	Rate constant(k ₂) (g mg ⁻¹ min ⁻¹)	0.024 [4]
Henry Nb-W complex	19.41 mg/g 1	Rate constant 10 ppm	4.998 [5]
Tyrosin	0.919		
Langmuir nanocomposite	48.7 mg/g 0.996	q _m (mg g ⁻¹ ppm)	39.06 This work

Table S2.

		b (L mg ⁻¹)	10.7
Freundlich	0.904		

References

- [1] Y. Yao, F. Xu, M. Chen, Z. Xu, and Z. Zhu, “Adsorption behavior of methylene blue on carbon nanotubes,” *Bioresour. Technol.* 101, (2010) 3040–3046. doi: <https://doi.org/10.1016/j.biortech.2009.12.042>.
- [2] T. Liu *et al.*, “Adsorption of methylene blue from aqueous solution by graphene,” *Colloids Surfaces B Biointerfaces.* 90 (2012) 197–203. doi: <https://doi.org/10.1016/j.colsurfb.2011.10.019>.
- [3] A. Badri, I. Alvarez-Serrano, M. Luisa López, and M. Ben Amara, “Sol-gel synthesis, magnetic and methylene blue adsorption properties of lamellar iron monophosphate KMgFe(PO₄)₂,” *Inorg. Chem. Commun.* 121 (2020) 108217. doi: <https://doi.org/10.1016/j.inoche.2020.108217>.
- [4] P. Su *et al.*, “Hydroxylation of electrolytic manganese anode slime with EDTA-2Na and its adsorption of methylene blue,” *Sep. Purif. Technol.* 278, (2021) 119526. doi: <https://doi.org/10.1016/j.seppur.2021.119526>.
- [5] J. Yu, Y. Han, H. Jong, H. I. Jong, and G. Ra, “Two-step hydrothermal synthetic method of niobium-tungsten complex oxide and its adsorption of methylene blue,” *Inorganica Chim. Acta.* 507 (2020) 119562. doi: <https://doi.org/10.1016/j.ica.2020.119562>.
- [6] A. Kołodziejczak-Radzimska, A. Budna, F. Ciesielczyk, D. Moszyński, and T. Jesionowski, “Laccase from *Trametes versicolor* supported onto mesoporous Al₂O₃: Stability tests and evaluations of catalytic activity,” *Process Biochem.* 95 (2020) 71–80. doi: <https://doi.org/10.1016/j.procbio.2020.05.008>.
- [7] G. Aydoğdu Tığ, D. Koyuncu Zeybek, S. Pekyardimci, and E. Kılıç, “A novel amperometric biosensor based on ZnO nanoparticles-modified carbon paste electrode for determination of glucose in human serum,” *Artif. Cells Nanomed. Biotechnol.* (2012) 1–7.